ARP2/3-mediated junction-associated lamellipodia control VE-cadherin–based cell junction dynamics and maintain monolayer integrity

Abdallah Abu Taha, Muna Taha, Jochen Seebach, and Hans-J. Schnittler
Institute of Anatomy and Vascular Biology, WWU-Münster, 48149 Münster, Germany

ABSTRACT **Maintenance and remodeling of endothelial cell junctions critically depend on the VE-cadherin/catenin complex and its interaction with the actin filament cytoskeleton. Here we demonstrate that local lack of vascular endothelial (VE)-cadherin at established cell junctions causes actin-driven and actin-related protein 2/3 complex (ARP2/3)–controlled lamellipodia to appear intermittently at those sites. Lamellipodia overlap the VE-cadherin–free adjacent plasma membranes and facilitate formation of new VE-cadherin adhesion sites, which quickly move into the junctions, driving VE-cadherin dynamics and remodeling. Inhibition of the ARP2/3 complex by expression of the N-WASP (V)CA domain or application of two ARP2/3 inhibitors, CK-548 and CK-666, blocks VE-cadherin dynamics and causes intercellular gaps. Furthermore, expression of carboxy-terminal–truncated VE-cadherin increases the number of ARP2/3-controlled lamellipodia, whereas overexpression of wild-type VE-cadherin largely blocks it and decreases cell motility. The data demonstrate a functional interrelationship between VE-cadherin–mediated cell adhesion and actin-driven, ARP2/3-controlled formation of new VE-cadherin adhesion sites via intermittently appearing lamellipodia at established cell junctions. This coordinated mechanism controls VE-cadherin dynamics and cell motility and maintains monolayer integrity, thus potentially being relevant in disease and angiogenesis.**

Monitoring Editor
Laurent Blanchoin
CEA Grenoble

Received: Jul 23, 2013
Revised: Oct 15, 2013
Accepted: Nov 7, 2013

This article was published online ahead of print in MBoC in Press (http://www.molbiolcell.org/cgi/doi/10.1091/mbc.E13-07-0404) on November 13, 2013.

A.A.T. performed and designed most of the experimentations and analyses. M.T. did the quantitative VE-cadherin expression studies. J.S. developed the software used and performed the quantification of fluorescence images. H.S. supervised all work and wrote the manuscript.

The authors declare no competing financial interests.

Address correspondence to: Hans Schnittler (hans.schnittler@uni-muenster.de).

Abbreviations used: ARP2/3 complex, actin-related protein 2/3 complex; Cdc42, cell division control protein 42 homologue; EGFP, enhanced green fluorescent protein; EGFP-p20, p20 tagged to EGFP; Ena/Vasp, enabled/vasodilator-stimulated phosphoprotein; GTPases, guanosine-5′-triphosphatease; HUVEC, human umbilical vein endothelial cells; JAIL, junction-associated intermittent lamellipodia; mDia1, mouse Diaphanous-related formin-1; NPFs, nucleation-promoting factors; N-WASP, neuronal-Wiskott–Aldrich syndrome protein; Rac1, Ras-related C3 botulinum toxin substrate 1; SCAR/WAVE, suppressor of cAR/ WASP family verprolin-homologous protein; TNF-α, tumor necrosis factor-α; (V)CA, verpolin homology, cofilin homology, acidic region; VE-cadherin, vascular endothelial-cadherin; VE-cadherin-EGFP, VE-cadherin tagged to EGFP; VE-cadherin-mCherry, VE-cadherin tagged to mCherry; WH2, Wiskott–Aldrich syndrome homology region 2.

INTRODUCTION

Intercellular junctions of the vascular endothelium are believed to be critical regulators in tissue development, sheet migration, body compartmentalization, cell polarity, and cell proliferation and are essential targets in inflammation, wound healing, and angiogenesis (Dejana *et al*., 2009; Vestweber *et al*., 2009). To fulfill these challenging functions, endothelial junctions must react quickly and be highly dynamic. Apart from tight and gap junctions, the adherens junctions provide the structural and functional backbone of endothelial junctions, as they are essential to establishing a barrier and are ubiquitously expressed irrespective of organ and vascular segments (Simionescu *et al*., 1975, 1976). Adherens junctions consist of vascular endothelial (VE)-cadherin, which binds $p120^{ctn}$ and β- or γ-catenin in a mutually exclusive manner; further binding to α-catenin forms the VE-cadherin/catenin complex, which interacts with junction-associated actin filaments (Suzuki *et al*., 1991; Lampugnani *et al*., 1992). Antibody labeling of the VE-cadherin/catenin complex reveals two different patterns. A continuous line of VE-cadherin is characteristically seen in vivo (Geyer *et al*., 1999; Adamson *et al*., 2002), in highly confluent cell cultures (Lampugnani *et al*., 1995), and

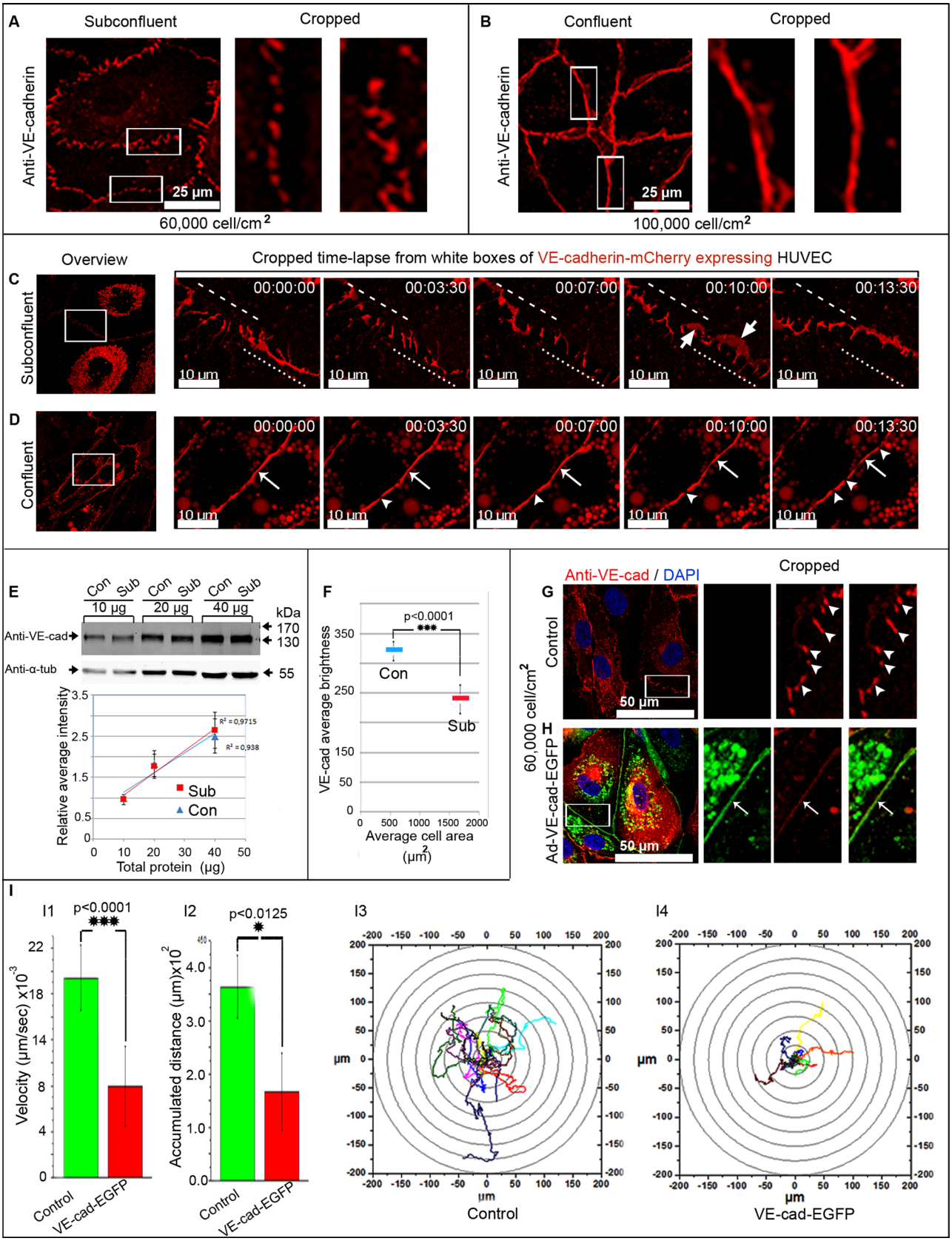

FIGURE 1: VE-cadherin distribution and dynamics are cell-density dependent. (A, B) Native (A) subconfluent and (B) confluent HUVEC cultures were labeled with anti-VE-cadherin, which appears interrupted in subconfluent cultures, whereas confluent ones display a continuous line. (C, D) Time-lapse recordings of VE-cadherin-mCherry–expressing HUVEC. (C) Subconfluent cultures display a permanent change in VE-cadherin patterning. Overlapping VE-cadherin adhesion sites are marked (large arrows). (D) Confluent HUVEC mostly exhibit a continuous VE-cadherin distribution

particularly after shear stress or hydrocortisone stimulation (Schrot *et al.*, 2005; Seebach *et al.*, 2007). In contrast, interrupted VE-cadherin patterning predominates in subconfluent growing cultures (Lampugnani *et al.*, 1995) and is also characteristically found at junctions of migrating endothelial cells during wound healing and after application of inflammatory mediators such as tumor necrosis factor-α (TNF-α) (Wahl-Jensen *et al.*, 2005; McKenzie and Ridley, 2007). These phenomena are accompanied by cellular shape change, increased cell motility, loss of junction-associated actin filaments, and formation of stress fibers (Lamalice *et al.*, 2007; Pober and Sessa, 2007; Yuan and He, 2012). The ability of certain stimuli to cause VE-cadherin remodeling, which is accompanied by changes in paracellular barrier function, has been relatively well described and involves phosphatases, kinases, and Rho GTPases (Dejana *et al.*, 2009; Vestweber *et al.*, 2009; Beckers *et al.*, 2010). However, coordinated activity between actin and VE-cadherin dynamics at established cell junctions has been less investigated, particularly in endothelium. In contrast, initial formation of cell junctions is well understood; this is mediated by actin-driven lamellipodia that bring adjacent cells together, allowing cell adhesion receptors to bind and causing formation of cell adhesion complexes (Nelson, 2008; Noda *et al.*, 2010; Baum and Georgiou, 2011; Yonemura, 2011; Hoelzle and Svitkina, 2012). Many actin-regulating proteins control actin assembly even at cadherin adhesion sites. These include Ena/Vasp, the small GTPases Rac1 and Cdc42 (Kim *et al.*, 2000; Kovacs *et al.*, 2002; Scott *et al.*, 2006; Kitt and Nelson, 2011), actin nucleation proteins such as actin-related protein 2/3 complex (ARP2/3) and formins such as mDia1 (Kovacs *et al.*, 2002; Kobielak *et al.*, 2004; Carramusa *et al.*, 2007), and class I nucleation-promoting factors (NPFs) such as N-WASP and SCAR/WAVE (Vasioukhin *et al.*, 2000; Helwani *et al.*, 2004), and cortactin that belongs to classII NPF (Welch and Mullins, 2002). The ARP2/3 complex facilitates cadherin engagement and junction formation (Nelson, 2008; Noda *et al.*, 2010; Baum and Georgiou, 2011; Yonemura, 2011; Hoelzle and Svitkina, 2012) and competes with α-catenin dimers for actin binding at cell junctions (Drees *et al.*, 2005; Yamada *et al.*, 2005). In epithelium the ARP2/3 complex is crucial in establishing adherens junctions, a process that requires Rac signaling (Brieher and Yap, 2013). Junction formation in endothelium and epithelium follows the same mechanisms, with the exception that endothelial cells display a transition from lamellipodia to filopodia, resulting in discontinuous VE-cadherin patterning in growing cell cultures (Hoelzle and Svitkina, 2012). This type of junction is described as being highly dynamic, while a continuous pattern of VE-cadherin, as seen in confluent cells and in endothelium in vivo, is characterized as being stable (Geyer *et al.*, 1999; Millan *et al.*, 2010; Huveneers *et al.*, 2012). Identification of the mechanisms and principles that drive and coordinate VE-cadherin and actin dynamics is the main topic of this work.

RESULTS

Cell density–dependent VE-cadherin dynamics

Confocal laser microscopy localized immunolabeled VE-cadherin at the junction of human umbilical vein endothelial cell (HUVEC) cultures in two forms: a zigzagged, interrupted, punctuate form, which was mostly prominent in subconfluent cultures, and extended VE-cadherin clusters appearing as continuous lines, which were predominant in confluent cells (Figure 1, A and B). To investigate the dynamic regulation of VE-cadherin/catenin complex in endothelial cells, full-length VE-cadherin was carboxy-terminally tagged with mCherry (VE-cadherin-mCherry) and expressed in HUVEC. VE-cadherin-mCherry displayed the expected molecular weight of 160–170 kDa (Supplemental Figure S1A), precipitated and colocalized with native VE-cadherin and catenins in a random manner at the cell junctions of both HUVEC and VE-cadherin–knockout endothelioma cells (Supplemental Figure S1, B–D), and responded to a calcium shift (Supplemental Figure S2A and Supplemental Video S1). In a first experimental setup, the dynamics of VE-cadherin-mCherry was studied by live-cell imaging in subconfluent ([6–9] $\times$ 10^4 cells/cm^2) and confluent cultures ([9–10] $\times 10^4$ cells/cm^2) using a special plating assay (for details see Supplemental Material and Methods and Supplemental Figure S2B). Consistent with VE-cadherin in native cells (Figure 1, A and B), VE-cadherin-mCherry appeared characteristically in two forms: as an interrupted pattern mostly present in subconfluent cultures and as VE-cadherin continuous lines (Supplemental Figure S2C). Time-lapse recording revealed repetitive VE-cadherin-mCherry remodeling, with continuous transitions between the interrupted and continuous patterning (Figure 1C and Supplemental Video S2). A transient appearance of VE-cadherin-mCherry–positive plaque-like structures regularly occurred (Supplemental Video S2). Transitions decreased with increasing cell density, and the continuous VE-cadherin-mCherry patterning became predominant. However, VE-cadherin-mCherry dynamics persisted even in highly confluent cultures (Figure 1D and Supplemental Video S2).

To better understand the background of the different VE-cadherin patterning, we determined both the junction-localized relative and the total amount of VE-cadherin in subconfluent and confluent HUVEC cultures. Of interest, the relative VE-cadherin amount at cell junctions was significantly less in subconfluent than in confluent cultures (Figure 1F and Supplemental Figure S2, D and E), whereas the total amount of VE-cadherin remained constant (Figure 1E), a result that confirms an earlier report (Lampugnani *et al.*, 1995). As a

(small arrows) with very small interruptions (arrowheads; see also Supplemental Figure S1 and Supplemental Videos S1 and S2). Dynamic translocating junctions are indicated by dotted and dashed lines. (E–I) The relative junction-localized VE-cadherin concentration, but not the total amount of VE-cadherin, is cell-density dependent. (E) Western blot analyses of VE-cadherin taken from subconfluent and confluent HUVEC cultures. Different amounts of total cellular protein (10, 20, and 40 µg) were probed by anti–VE-cadherin, followed by densitometry and determination of r^2. α-Tubulin served as an internal loading control. $n = 3$ independent dual-probe experiments (see also Supplemental Figure S2). (F) The relative junction-localized VE-cadherin concentration was determined by a quantification of the average brightness of cell junctions by a defined ROI plotted against average cell area (for details compare Supplemental Figure S2, C–E). Altogether 434 confluent cells and 75 subconfluent cells from three independent experiments were analyzed ($p < 0.0001$). (G–I) Overexpression of VE-cadherin-EGFP in subconfluent HUVEC cultures (~6×10^4 cells/cm^2) down-regulates cell motility. (G, H) Immunolabeling of VE-cadherin in (G) native subconfluent HUVEC discloses the typical interrupted patterning, whereas (H) VE-cadherin-EGFP–overexpressing subconfluent HUVEC displayed a continuous line. (I) Quantification of the cell motility of native and VE-cadherin-EGFP–overexpressing cells is indicated by (I1) cell velocity, (I2) accumulated distance, and (I3, I4) track plots. Quantification was performed on 15 cells from 200 frames acquired within 5 h and 50 min (see also Supplemental Video S3).

consequence, the limited amount of VE-cadherin distributes in large subconfluent cells with long cell junctions in an interrupted pattern. In contrast, the small confluent cells with short cell border length exhibit a continuous VE-cadherin distribution. Although appearing simple at first glance, this principle sufficiently explains the cell density–dependent VE-cadherin patterning and might also explain the high junction dynamics in less confluent cells. This is consistent with earlier studies in which the appearance of lamellipodia (ruffles, membrane protrusions) at endothelial junctions was described (Seebach *et al.*, 2005). Here we propose that the local VE-cadherin concentration is critical in control of junction dynamics, including lamellipodia formation.

To investigate this hypothesis, we increased the VE-cadherin concentration at cell junctions in subconfluent HUVEC cultures (6×10^4 cells/cm^2), cell culture conditions that display large and frequent lamellipodia formation at cell junctions and high cell motility. To maintain the subconfluent state of the culture, we used an adenovirus vector encoding VE-cadherin–enhanced green fluorescent protein (EGFP; Kametani and Takeichi, 2007), which caused quick overexpression within 12 h in HUVEC cultures. The lentiviral vector needs 2–3 d to increase VE-cadherin-mCherry expression moderately. This long time interval is accompanied by cell proliferation and thus precludes the use of the lentiviral vector for this experiment. Indeed, the overexpressed VE-cadherin-EGFP localized in a continuous line along the junctions (Figure 1H) in subconfluent cultures ([6–9] $\times 10^4$ cells/cm^2), whereas control cultures still exhibited the interrupted patterning (Figure 1G). The effect of VE-cadherin overexpression on cell dynamics and lamellipodia formation was then investigated by time-lapse phase contrast microscopy. In line with earlier results (Seebach *et al.*, 2005), HUVEC cultures show high cell motility and lamellipodia formation at cell junctions (Supplemental Video S3). Consistent with our hypothesis, both cell motility and lamellipodia formation decreased in VE-cadherin-EGFP–overexpressing HUVEC cultures (Figure 1I and Supplemental Video S3). Cell motility was determined by cell track plots, measuring cell velocity and accumulated distance (Figure 1I). The data show that the level of VE-cadherin expression at the junctions determines lamellipodia formation, which in turn seems to be important in total cell motility. Because lamellipodia formation requires actin polymerization, our goal was to understand the actin dynamics at endothelial cell junctions by live-cell imaging using LifeAct-EGFP.

Actin dynamics at cell junctions

LifeAct-EGFP (Riedl *et al.*, 2008) was cloned into a lentiviral vector and expressed in HUVEC cultures. The expressed fusion protein displayed the expected molecular weight and bound to actin filaments, as it colocalized with phalloidin-rhodamine–labeled actin filaments (Supplemental Figure S3, A and B). Live-cell imaging revealed the characteristic actin-driven lamellipodia at leading edges of single cells (Figure 2A and Supplemental Video S4). Of importance, actin-driven, junction-associated lamellipodia still occurred intermittently at established junctions in subconfluent (Figure 2B and Supplemental Video S4) and even in confluent cultures (Figure 2C and Supplemental Video S4). Owing to their temporal and spatial appearance, these structures are defined as junction-associated intermittent lamellipodia (JAIL). The size and the number of JAIL decreased with increased cell density (see later discussion).

As demonstrated, overexpression of VE-cadherin-EGFP led to down-regulation of junction-associated intermittent and actin-driven lamellipodia. Taking into consideration that the ARP2/3 complex competes for actin binding with α-catenin, a main component of the cadherin/catenin complex (Drees *et al.*, 2005; Yamada *et al.*, 2005), we investigated the dynamics of ARP2/3 at cell junctions of the endothelium. Thus the p20 subunit of the heptameric ARP2/3 complex tagged at the amino terminus with EGFP (Kaverina *et al.*, 2003) was subcloned into the lentiviral vector and expressed in HUVEC cultures.

The ARP2/3 complex drives formation of junction-associated intermittent lamellipodia in a cell density–dependent way

EGFP-p20 expressed in HUVEC displayed the expected molecular weight of 47 kDa (Supplemental Figure S3C), and an anti-EGFP antibody precipitated the ARP3 subunit (Supplemental Figure S3D). EGFP-p20 was incorporated into the endogenous ARP2/3 complex and colocalized with ARP2, ARP3, and actin filaments at lamellipodia (Supplemental Figure S3, E and F, and Supplemental Video S5). However, we found a cell density–dependent appearance and persistent formation of JAIL in all HUVEC cultures (Figure 2, D and E, and Supplemental Video S6). In subconfluent cell cultures (6×10^4 cells/cm^2) JAIL are large, having a mean size of 48 μm^2 (Figure 2G) and a mean duration of 5 min (Figure 2H), whereas confluent cultures (up to 1×10^5 cells/cm^2) displayed reduced JAIL, with a mean size of 29 μm^2 and a reduced mean duration of 3.5 min (Figure 2, F–H). JAIL formation in confluent cultures appeared as flickering points of light in time-lapse videos (Supplemental Video S6), a result not seen in fixed cells due to the short duration and low frequency of JAIL. Taken together, the spatiotemporal dynamics of both VE-cadherin-mCherry and p20-EGFP suggest an interdependent relationship between VE-cadherin–mediated cell adhesion and ARP2/3-controlled JAIL formation.

New VE-cadherin adhesion sites develop dynamically due to formation of JAIL, which in turn is controlled by the local VE-cadherin concentration

The functional relationship between VE-cadherin and ARP2/3 complex–controlled JAIL formation was investigated by coexpression of VE-cadherin-mCherry and EGFP-p20 in HUVEC cultures. Both the protein dynamics and cellular distribution of coexpressed proteins were similar to the case in which fusion proteins were expressed alone. ARP2/3-containing JAIL preferentially developed at gaps between and close to VE-cadherin clusters (Figure 3A and Supplemental Video S7), which is further verified in unmodified HUVEC by antibody labeling (Supplemental Figure S4, B and C). ARP2/3 complex–positive JAIL preferentially appeared at interruptions between and close to the VE-cadherin/catenin complex (Supplemental Figure S4, D–G). JAIL overlapped plasma membranes of adjacent cells, which generally facilitated the formation of VE-cadherin-mCherry adhesion plaques, followed by clustering and subsequent incorporation into the cell borders (Figure 4A and Supplemental Video S8). This process changed the VE-cadherin-mCherry patterning, a process that explains the highly dynamic VE-cadherin-mCherry remodeling in subconfluent cultures, whereas confluent cultures display less JAIL due to increased VE-cadherin concentration (Figure 3, B and B1, and Supplemental Video S7), as already described (Figure 1, G and H, and Supplemental Video S3). However, to further verify this concept, we expressed VEcad-ΔC164mCherry in HUVEC. This carboxy-terminal–deleted mutant is unable to bind β- or γ-catenins or p120^{ctn} and thus is disconnected from junction-localized actin filaments. Expressed VE-cad-ΔC164-mCherry displayed the expected molecular weight (Supplemental Figure S5A) and localized randomly at cell junctions in HUVEC cultures (Figure 4B), indicating sufficient incorporation of the mutant. Those cell cultures exhibit increased

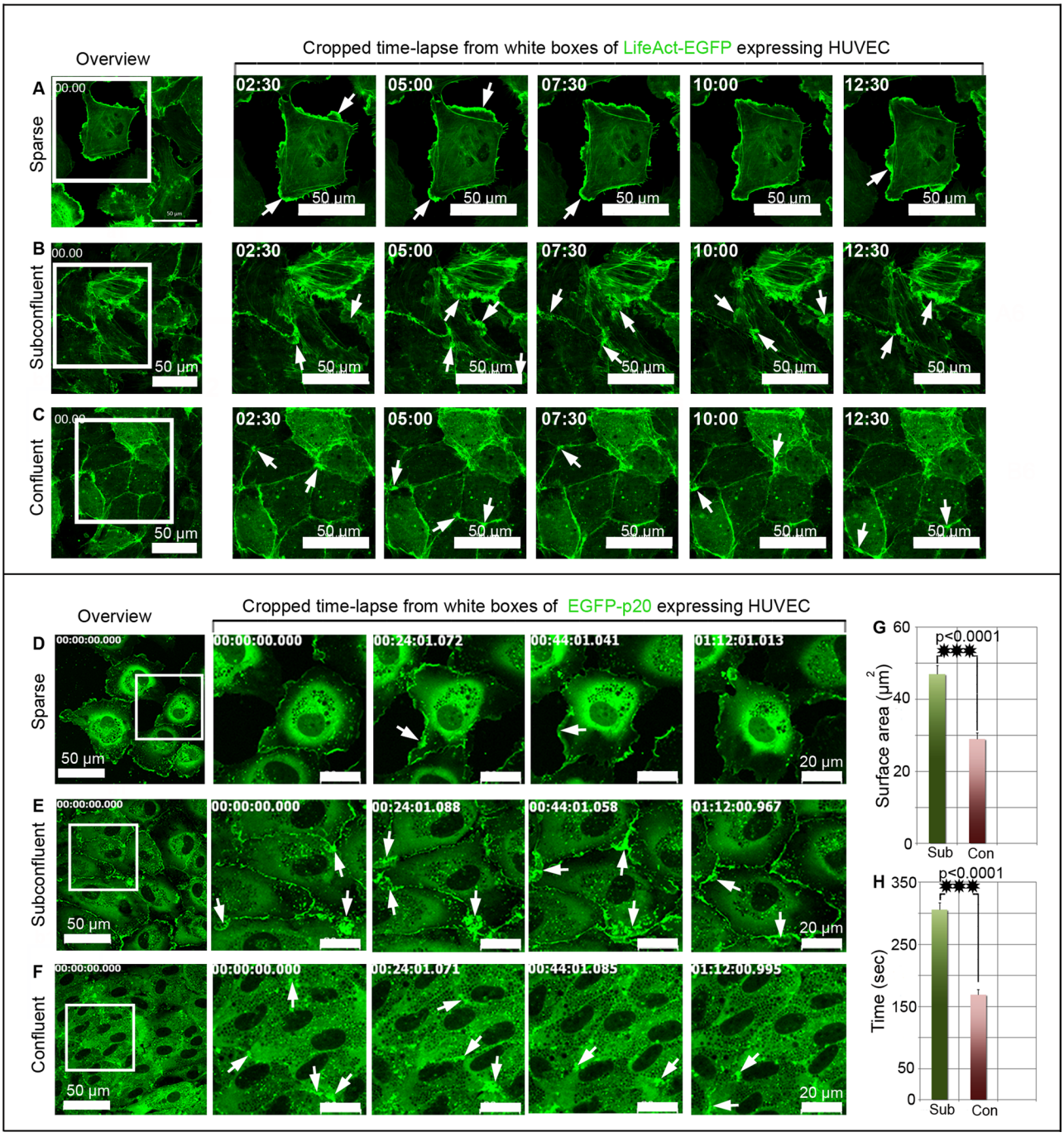

FIGURE 2: Cell density–dependent actin and ARP2/3 complex dynamics at endothelial junctions. (A–C) LifeAct-EGFP and (D–F) EGFP-p20 were expressed in HUVEC cultures, and time-lapse recordings were performed at culture areas showing different cell densities within the same culture. (A–C) Left, overviews; white boxes indicate cropped and enlarged areas. (A) LifeAct-EGFP dynamics at lamellipodia (arrows) of single cells. (B) Large LifeAct-EGFP–positive and junction-associated lamellipodia (arrows) develop in subconfluent cells intermittently, whereas (C) only small ones (arrows) appear in confluent cultures (see also Supplemental Video S4). (D–F) Left, overviews; white boxes indicate cropped and enlarged areas. (D) EGFP-p20 dynamics is typically seen at lamellipodia (arrows) of single cells. (E) Large EGFP-p20–positive junction-associated lamellipodia (arrows) intermittently appear at junctions of subconfluent cells, whereas smaller ones are present in confluent cultures (see also Supplemental Video S6). (G, H) Quantification of lamellipodia size and duration in subconfluent (Sub) and confluent cultures (Con). Two hundred cells of both confluent and subconfluent culture were analyzed from $n = 5$ independent experiments. ***$p < 0.0001$. See also Supplemental Figure S2 and Supplemental Videos S4–S6.

formation of JAIL by about fourfold (Figure 4, C–E, and Supplemental Video S9), a result totally in line with decreased JAIL formation in VE-cadherin-mCherry–overexpressing cultures (Figure 1, G and H, and Supplemental Video S3). These data show that the VE-cadherin patterning and concentration at cell junctions determine JAIL formation.

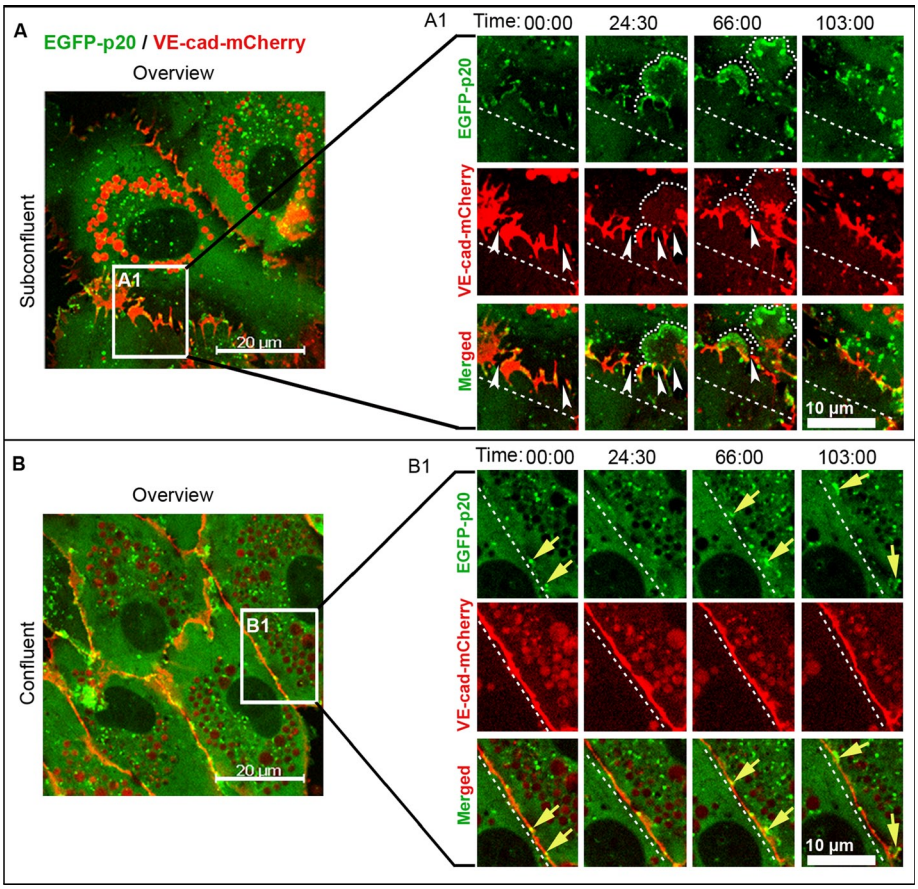

FIGURE 3: ARP2/3-controlled JAIL develop at spaces between VE-cadherin clusters in a cell density–dependent manner. (A, B) Time-lapse recording (min:s) of EGFP-p20 (green) and VE-cadherin-mCherry (red) coexpressed in (A, A1) subconfluent and (B, B1) confluent HUVEC cultures. (A, B) Overviews; white boxes indicate cropped and magnified areas. (A1) Large, EGFP-p20 positive JAIL (dotted curved lines) of subconfluent cultures are prominent at interruption (white arrowheads) between VE-cadherin-mCherry clusters. (B1) Only small JAIL (yellow arrows) are visible at small VE-cadherin-mCherry interruptions in confluent HUVEC cultures. Dashed lines indicate reference lines in order to visualize translocating junctions. Frames are representative of 20 independent experiments with subconfluent cultures and 15 experiments using confluent cultures. See also Supplemental Figure S4 and Supplemental Video S7.

ARP2/3 complex–mediated JAIL formation maintains endothelial monolayer integrity

We next considered whether the ARP2/3 complex modulates the overall VE-cadherin dynamics. Therefore the (V)CA domain (amino acids 430–505) of the nucleation-promoting factor N-WASP, which acts as a dominant-negative mutant that blocks ARP2/3 activity (Pollard, 2007; Rottner *et al.*, 2010), was fused to m-Cherry (mCherry-(V)CA; Supplemental Figure S5A2). Expression of mCherry-(V)CA (Figure 5A) in HUVEC reduced stress fibers, caused intercellular gaps, and recruited the VE-cadherin/catenin complex to a small, faint line at the cell junctions, as verified by colabeling of α-catenin and filamentous actin (Figure 5A). Live-cell imaging showed reduced JAIL formation in mCherry-(V)CA–expressing cells accompanied by largely blocked cell motility (Supplemental Video S10). For further verification, the quick-acting, and highly specific, ARP2/3 inhibitors CK-666 and CK-548 were used. CK-666 specifically binds to both ARP2 and ARP3 subunits and locks the ARP2/3 complex in its inactive conformation (Hetrick *et al.*, 2013). CK-548 specifically binds to the hydrophobic core of ARP3 and thus blocks ARP2/3 complex activation in living cells (Nolen *et al.*, 2009).

Application of inactive inhibitor to HUVEC, CK-689 or CK-312 (Figure 5B and Supplemental Figure S5B), had no effect, whereas both 200 µM of the active CK-666 (Figure 5B) and 60 µM of the active inhibitor CK-548 (Supplemental Figure S5B) caused intercellular gaps. Furthermore, actin filament patterning was altered. The interdependent dynamics between VE-cadherin and JAIL was studied by live-cell imaging of HUVEC expressing VE-cadherin-mCherry together with either EGFP-p20 or LifeAct-EGFP. Both CK-666 and CK-548 caused intercellular gap formation and decreased VE-cadherin-mCherry dynamics (Figure 5C, Supplemental Figure S5C, and Supplemental Videos S11 and S12). Washing out of the active inhibitors quickly restored JAIL formation, a process that quickly closed intercellular gaps via newly formed VE-cadherin-mCherry–mediated cell adhesion sites (Figure 5C, Supplemental Figure S5C, and Supplemental Videos S11 and S12). This process increased VE-cadherin dynamics and demonstrates a critical role of the ARP2/3 complex in VE-cadherin patterning and dynamics. We conclude that the interdependent activity between ARP2/3-controlled lamellipodia formation and VE-cadherin–mediated cell adhesion allows a quick-acting, high plasticity of adherens junctions, a mechanism that also maintains endothelial monolayer integrity.

DISCUSSION

The endothelium, in particular cell junctions, exhibits high plasticity and quickly responds to certain stimuli, such as fluid shear stress, inflammatory mediators, wound healing, and angiogenesis. Plasticity requires distinct junction dynamics for remodeling, changes in paraendothelial barrier function, cell spreading, and cell migration. These processes depend on a balanced regulation between cell adhesion and remodeling and essentially rely on both the cadherin/catenin complex and the associated actin filaments (Weis and Nelson, 2006; Cavey and Lecuit, 2009; Yonemura, 2011). However, it has been unclear how the two components of this complex are spatially and temporally coordinated to regulate junction plasticity and adhesion and, at the same time, control barrier function.

On the basis of the data presented here, we propose an interdependent control cycle between VE-cadherin–mediated cell adhesion and ARP2/3-controlled and actin-driven JAIL formation, which drives VE-cadherin dynamics and allows plasticity (Figure 6). The proposed mechanism permits concurrent junction dynamics and cell adhesion and can explain the ability of cell junctions to respond to stimulation at different spatiotemporal scales. Such conditions include increasing and decreasing cell density and shape change, which are both accompanied by large variations in cell perimeter. Examples of this are cell elongation due to fluid shear stress stimulation (Levesque and Nerem, 1985; Seebach *et al.*, 2007) or after application of TNF-α (McKenzie and Ridley, 2007), during wound healing (Ichijima *et al.*, 1993), and during angiogenesis (Hetheridge *et al.*, 2012).

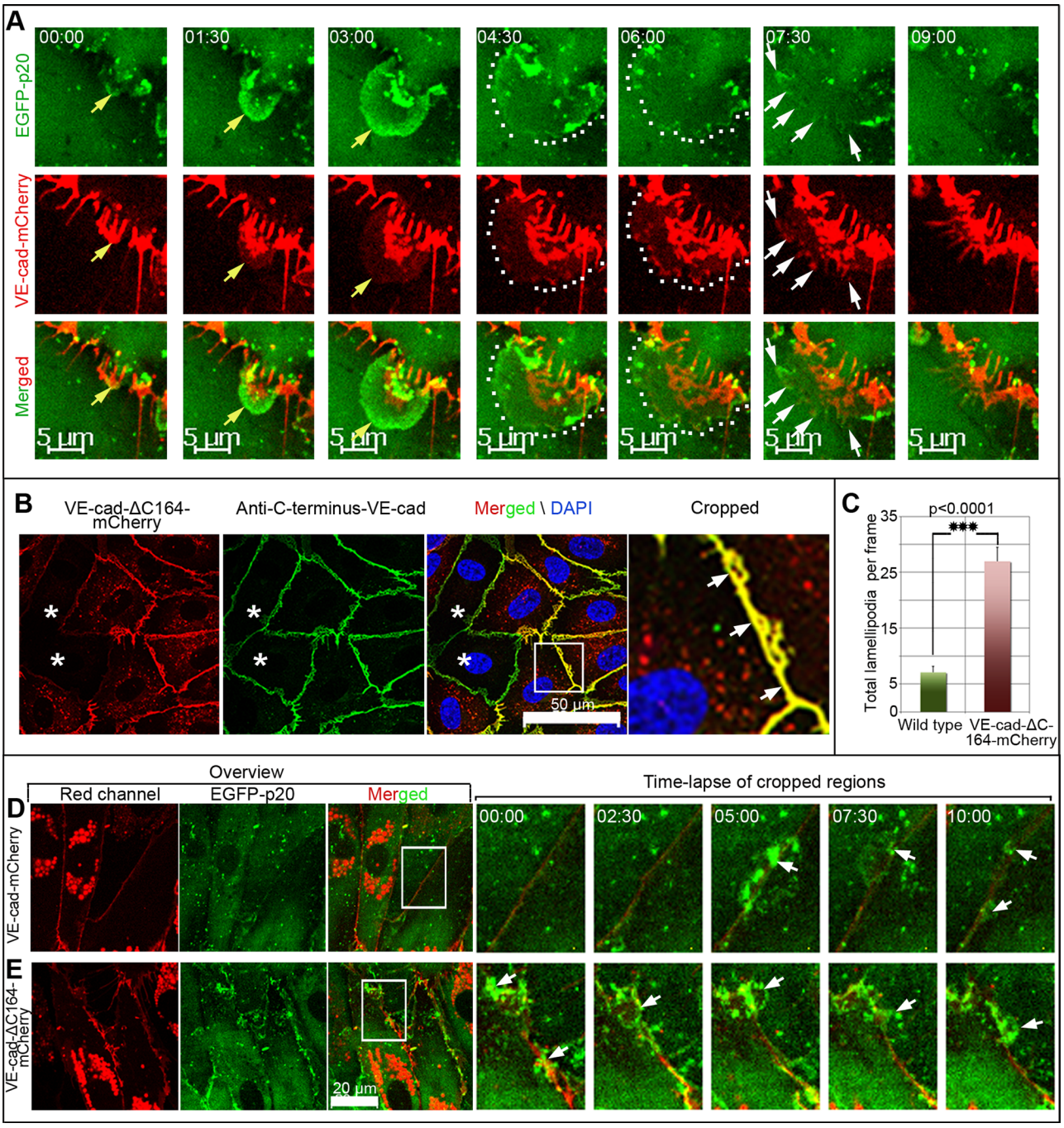

FIGURE 4: New VE-cadherin adhesion sites develop dynamically due to formation of JAIL, which are in turn controlled by the local VE-cadherin concentration. (A) Time-lapse series, taken from Supplemental Video S8, which shows a growing JAIL (top, yellow arrows), which induces new VE-cadherin-mCherry plaques (encircled by dotted lines) that cluster increasingly (white arrows) during JAIL retraction and assembly at cell junctions. See also Supplemental Figure S3 and Supplemental Video S8. (B) HUVEC cultures expressing VE-cad-ΔC164-mCherry (red) were labeled by an antibody specific to the carboxy-terminal domain of VE-cadherin (green), which demonstrated random incorporation of the mutant into the junctions (arrows in cropped and enlarged area). Stars indicate nontransduced cells. Nuclei are labeled by 4′,6-diamidino-2-phenylindole (blue). (C) Quantification of JAIL in subconfluent HUVEC cultures (6×10^4 cells/cm^2) expressing either VE-cadherin-mCherry and EGFP-p20 or VE-cad-ΔC164-mCherry and EGFP-p20, as indicated. (D, E) Time-lapse series of cropped areas (white boxes in the merged overview). As indicated, this demonstrates increased JAIL formation in VE-cad-ΔC164-mCherry–expressing HUVEC. Images depict one of three independent experiments. See also Supplemental Video S9.

The interdependence between VE-cadherin–mediated cell adhesion and ARP2/3-controlled and actin-driven JAIL is based on a relatively constant VE-cadherin expression for a given endothelial cell type, irrespective of cell size and density (Lampugnani *et al.*, 1995; this study). The natural principle behind this observation is elegant and yet simple. A given amount of VE-cadherin distributes

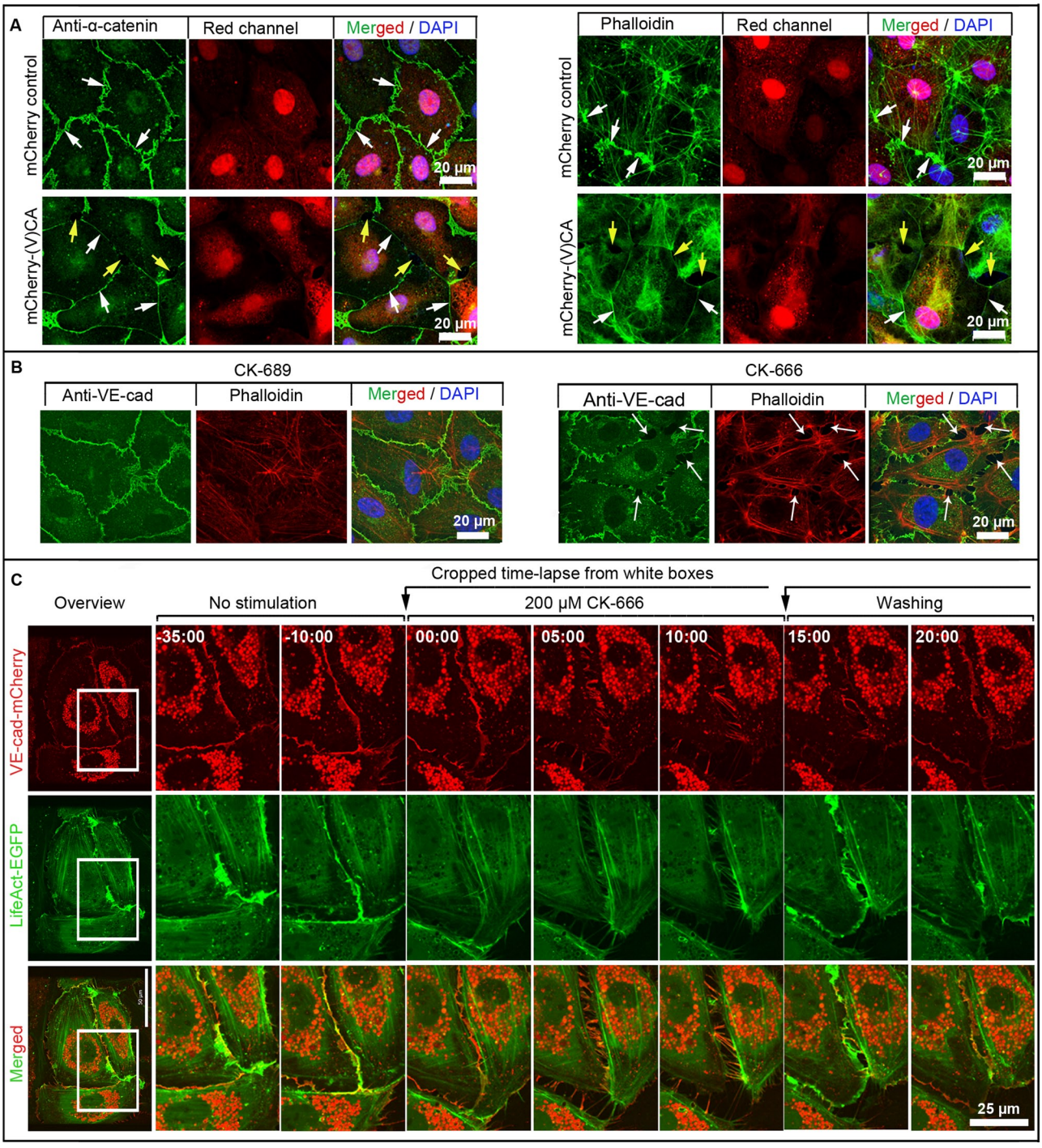

FIGURE 5: ARP2/3-controlled JAIL maintaining endothelial monolayer integrity. (A) HUVEC expressing either mCherry for control (red, top) or the mCherry-(V)CA domain (red, bottom), which was labeled with anti–α-catenin or phalloidin–Alexa Fluor 488, as indicated. Control HUVEC cultures exhibit the characteristic α-catenin patterning with small JAIL (white arrows, top). Expression of the mCherry-(V)CA domain causes small and faint continuous α-catenin and actin labeling (white arrows, bottom) accompanied by gap formation (yellow arrows, bottom). Nuclei are labeled by 4′,6-diamidino-2-phenylindole (blue). See also Supplemental Video S10. (B) ARP2/3 complex inhibitor CK-666 causes intercellular gap formation. Native HUVEC were treated with either inactive inhibitor, CK-689, for control, or active inhibitor, CK-666, for ~15 min. This was followed by immunolabeling of VE-cadherin (green) and actin filaments with phalloidin–tetramethylrhodamine isothiocyanate (red). CK-666–treated cultures exhibit interendothelial gaps (arrows) accompanied by VE-cadherin and actin recruitment to cell junctions. Shown is one of three independent experiments that yielded similar results. (C) Overview (left) of HUVEC expressing both VE-cad-mCherry and EGFP-p20. Time-lapse series (right) of ARP2/3 inhibitor CK-666 treatment followed by washout, as indicated. The inhibitor caused intercellular gaps accompanied by VE-cadherin remodeling as it recovers after the washing out. Shown is one of three independent experiments that yielded similar results.

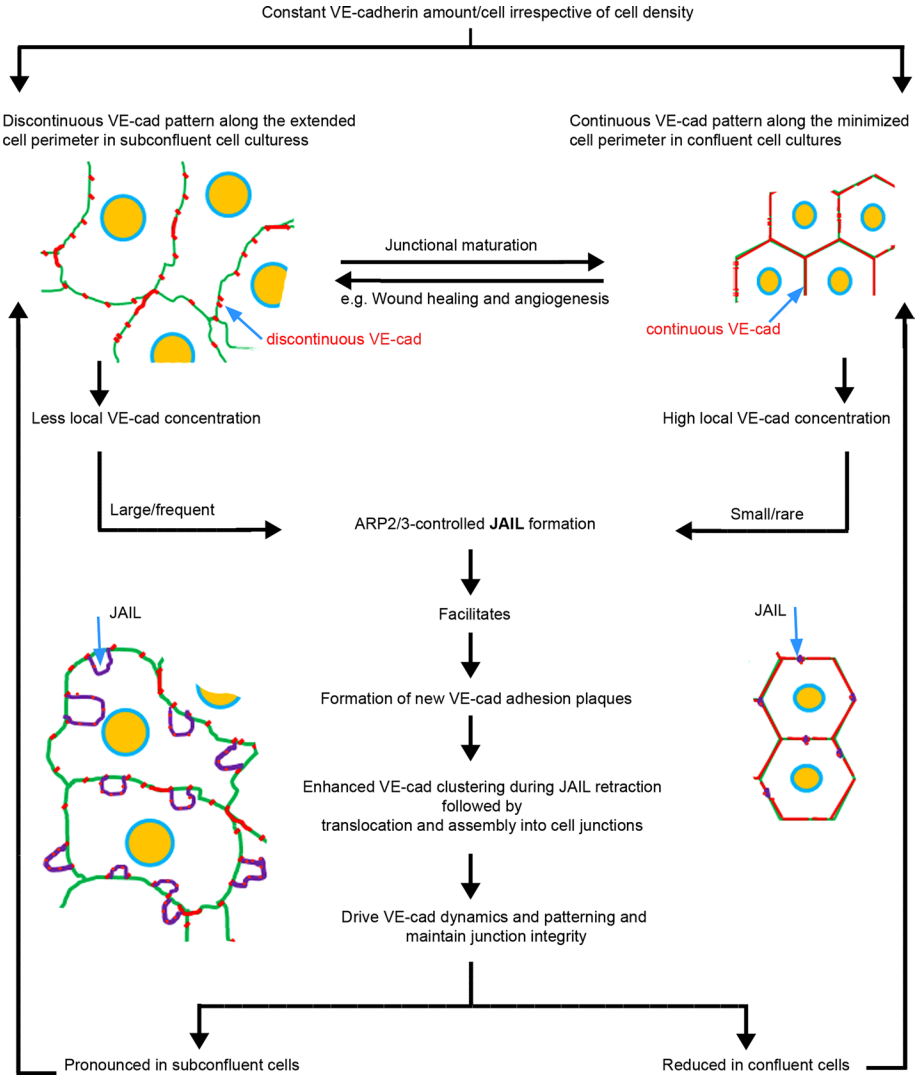

FIGURE 6: Scheme illustrating the interdependence between JAIL activity and VE-cadherin dynamics.

along the junctions. Consequently, long cell junctions of large cells, as seen in subconfluent cultures, display large VE-cadherin–free spaces between the individual VE-cadherin clusters. Increasing cell density reduces cell size and cell junction length, and thus VE-cadherin clusters fuse together to form a continuous line at the junctions. Because JAIL preferentially forms between VE-cadherin clusters, the presence of a continuous VE-cadherin distribution at the junctions reduces them. This concept is supported by overexpression of VE-cadherin-EGFP in subconfluent cell cultures, which display an interrupted VE-cadherin patterning and large JAIL under control conditions. VE-cadherin overexpression in those subconfluent cultures decreased both lamellipodia formation and cell motility. In contrast, expression of a carboxy-terminal deletion mutant increased the formation of junction-associated lamellipodia and dynamics. From an energy standpoint, this simple mechanism is very economical, as it does not necessarily require new protein synthesis.

The JAIL-induced new VE-cadherin adhesion sites became quickly incorporated into cell junctions, a mechanism that significantly changed the VE-cadherin pattern, and thus is a type of VE-cadherin dynamics. ARP2/3 complex activity also affects VE-cadherin distribution and integrity. In particular, inhibition of the ARP2/3 complex in subconfluent cells resulted in a faint, continuous line of VE-cadherin and was accompanied by formation of large intercellular gaps. It is reasonable to assume that the limited amount of VE-cadherin present in both confluent and subconfluent HUVEC cultures is responsible. Furthermore, inhibition of the ARP2/3 complex also modulated the actin filament patterning, such that it decreased the number of stress fibers. Because stress fibers can terminate at individual VE-cadherin clusters (Millan *et al.*, 2010) involving vinculin and develop mechanical strain (Huveneers *et al.*, 2012), they may contribute to VE-cadherin patterning as well.

The interdependent control between ARP2/3 activity and VE-cadherin–mediated cell adhesion has two important functional consequences: first, the formation of JAIL that appears between VE-cadherin clusters restores, at least to a certain degree, VE-cadherin adhesion sites, thus retaining at least a minimal barrier even in subconfluent cells. These results are in line with reports showing ARP2/3-dependent maintenance of the blood–testis barrier (Lie *et al.*, 2010) and sphingosine-1-phosphate–induced junction remodeling (Li *et al.*, 2004). Second, ARP2/3 activity maintains VE-cadherin dynamics and thus provides a source of junction plasticity under physiological and pathological conditions. It is reasonable to assume that a number of junction-controlling molecules, such as Rho GTPases, tyrosine kinases and phosphatases, cAMP, and protein kinase C, might cross-talk to the ARP2/3 complex directly or indirectly at cell junctions, but this has yet to be studied in detail. JAIL facilitated the generation of new VE-cadherin-mCherry adhesion sites at the overlapping plasma membrane of adjacent cells. This suggests that the cell surface contain VE-cadherin monomers and/or oligomers that might provide the source to rapidly form high-affinity adhesion sites, a phenomenon demonstrated for E-cadherin (Iino *et al.*, 2001). It is likely that there is a balance between formation and dissociation of VE-cadherin trans-adhesion complexes in a VE-cadherin concentration–dependent manner, but quantitative data supporting this assumption remain to be obtained.

Modulation of cadherin expression is critical in tissue formation during development, as frequently demonstrated for epithelium (Halbleib and Nelson, 2006). However, we showed a constant expression of total VE-cadherin in subconfluent and confluent endothelial cultures from the same source, in agreement with earlier reports (Lampugnani *et al.*, 1995). Irrespective of the possibility that VE-cadherin expression levels might vary within different vascular segments and organs, the principle of cell size–dependent distribution of VE-cadherin and in turn junction-associated lamellipodia formation at cell junctions still applies. This principle accounts for a number of novel aspects of junction regulatory mechanisms. For example, monolayer injury causes sheet migration associated with

cellular shape change and thus elongation of the cell perimeter, as described in vivo and in cell culture models (Rorth, 2009). Given that a particular stimulus does not change the total amount of cellular VE-cadherin in a particular environment or location (e.g., cell culture model, arteries, or veins), changes in shape and cellular perimeter cause both VE-cadherin remodeling (e.g., into an interrupted pattern, which modulates the dynamics) and changes in functional features of the cells, such as paracellular permeability and migration activity (Wu and Horowitz, 2011). Under these conditions, increased ARP2/3-mediated junction-associated lamellipodia can serve as a critical mechanism for controlling junction plasticity, a requirement for regulated regeneration. Thus this study expands the functional role of the ARP2/3 complex in VE-cadherin/catenin complex–mediated cell junction dynamics, plasticity, and monolayer integrity.

MATERIALS AND METHODS

Primers, antibodies, and reagents

Primers, antibodies, and reagents used in this study are listed and described in the Supplemental Materials and Methods (Supplemental Tables S1 and S2).

Cell culture

HUVEC and HEK 293T cells were cultured as described elsewhere (Kronstein *et al.*, 2012), and cells of the first passages were used. VE-cadherin–deficient endothelioma cells were obtained from the group of D. Vestweber that had been established from VE-cadherin$^{-/-}$ mouse embryos generated by the same laboratory. These cells were cultured as described elsewhere (Kronstein *et al.*, 2012). For further details, see the Supplemental Materials and Methods.

Immunofluorescence staining and antigen retrieval

Immunolabeling was performed under standard conditions. For ARP3 and p21 staining, cultures were subjected to antigen retrieval procedure (Shi *et al.*, 2011). For details, see the Supplemental Materials and Methods.

Cloning, recombinant lentiviruses, gene transduction, and live-cell imaging

The cDNA of mCherry or EGFP was fused to the C-terminus of full-length human VE-cadherin, C-terminally truncated (Δ164 amino acids) VE-cadherin, or LifeAct or the N-terminus of human N-WASP (V) CA domain or β-actin and subsequently cloned into the lentiviral vector (pFUGW). EGFP-p20 plasmid was kindly given by Theresia Stradal (WWU-Münster, Münster, Germany; Kaverina *et al.*, 2003). The construct was subcloned into the pFUGW vector. Generation of recombinant lentiviruses was followed by transduction into HUVECs as described elsewhere (Kronstein *et al.*, 2012). Cells were cultured until appropriate levels of protein expression were obtained. For all details, see the Supplemental Materials and Methods. Fluorescent live-cell imaging was performed by confocal spinning disk microscopy (Carl Zeiss, Göttingen, Germany) at 37°C and 5% CO_2. For details, see the Supplemental Materials and Methods.

Immunoprecipitation and Western blot analyses

Immunoprecipitation was performed as described elsewhere (Geyer *et al.*, 1999; Seebach *et al.*, 2007). Total immunoprecipitates or a defined amount of SDS-solubilized protein was loaded on the SDS gels and further subjected to Western blotting using the respective antibodies. Bands were quantified by near-infrared (NIR) secondary antibodies using a LICOR NIR scanner according to the manufacturer's instructions (LI-COR Biotechnology, Bad Homburg, Germany).

Quantification of total VE-cadherin in confluent and subconfluent cells

The total amount of SDS-solubilized protein of HUVEC cultures at a density of 10×10^4 cells/cm^2 for confluent or 6×10^4 cells/cm^2 for subconfluent cultures was determined by Amidoschwarz protein-determination assay (Dieckmann-Schuppert and Schnittler, 1997). Equal amounts of proteins were subjected to SDS-gel electrophoresis and subsequently processed for quantitative Western blot analysis. The average intensity of normalized values was plotted as a function of the amount of total protein. Regression analysis was performed with Excel (Microsoft, Redmond, WA).

Image analysis

Automated image analysis of proteins at cell junctions was performed according to a newly developed algorithm and software termed Cell Border Tracker (J. Seebach, J. Lenk, A. Abu Taha, X. Jiang and H.-J. Schnittler, unpublished data). The relative amount of VE-cadherin was measured by the average brightness of junction-localized VE-cadherin, defined by the total fluorescence intensity of a region of interest (ROI) divided by the area of the ROI. In two particular cases, however, manual selection of junction-associated lamellipodia was necessary. This includes expression of both EGFP-p20 and either the VE-cad-ΔC164-mCherry or VE-cadherin-mCherry. For details, see the Supplemental Materials and Methods.

Cell tracking based on phase contrast–acquired time-lapse series

For preprocessing, the gray levels of the phase contrast images were inverted and corrected for background intensity using ImageJ (National Institutes of Health, Bethesda, MD), public domain Java image processing and analysis software (Schneider *et al.*, 2012). In the resulting images, automated tracking of individual cells was performed using software developed at the Center for Biomedical Optics and Photonics, University of Münster (Münster, Germany), based on an algorithm as described elsewhere (Kemper *et al.*, 2010). The correctness of each migration trajectory was controlled by observing the detected cell positions in movies of the preprocessed phase images and comparing them to the initial phase contrast images.

Statistical analysis

Unpaired *t* tests were performed using GraphPad software (La Jolla, CA) available as an online calculator, QuickCalcs (www.graphpad.com/quickcalcs/ttest1). Data were considered statistically significant when $p < 0.05$. Error bars indicate SD.

ACKNOWLEDGMENTS

We thank Annelie Ahle and Angelika Vollmer for excellent technical assistance. We are grateful to Theresia Stradal (WWU-Münster, Münster, Germany) for human EGFP-p20 cDNA, Sunil K. Shaw (Brown University, Providence, RI) for human VE-cadherin cDNA, Beat A. Imhof (Center Medical Universitaire, Geneva, Switzerland) for β-actin cDNA, Dirk Lindemann (MTZ, Dresden, Germany) for mCherry antibody, Dietmar Vestweber (Max Plank Institute, Münster, Germany) for VE-cadherin–knockout endothelioma cells and discussion, and Till Rauterberg (Servicepunkt Film, WWU-Münster) for editing the videos. Björn Kemper provided the phase contrast–based tracking software, and we are grateful for his feedback. This work was supported by the Center for Regenerative Therapies Dresden, the Dresden International Graduate School for Biomedicine and Bioengineering (Dresden, Germany), and grants of the German Research Council, DFG INST 2105/24–1 and SCHN 430/6–1, to H.S.

REFERENCES

Adamson RH *et al.* (2002). Rho and Rho kinase modulation of barrier properties: cultured endothelial cells and intact microvessels of rats and mice. J Physiol 539, 295–308.

Baum B, Georgiou M (2011). Dynamics of adherens junctions in epithelial establishment, maintenance, and remodeling. J Cell Biol 192, 907–917.

Beckers CM, van Hinsbergh VW, van Nieuw Amerongen GP (2010). Driving Rho GTPase activity in endothelial cells regulates barrier integrity. Thromb Haemost 103, 40–55.

Brieher WM, Yap AS (2013). Cadherin junctions and their cytoskeleton(s). Curr Opin Cell Biol 25, 39–46.

Carramusa L, Ballestrem C, Zilberman Y, Bershadsky AD (2007). Mammalian diaphanous-related formin Dia1 controls the organization of E-cadherin-mediated cell-cell junctions. J Cell Sci 120, 3870–3882.

Cavey M, Lecuit T (2009). Molecular bases of cell–cell junctions stability and dynamics. Cold Spring Harb Perspect Biol 1, a002998.

Dejana E, Tournier-Lasserve E, Weinstein BM (2009). The control of vascular integrity by endothelial cell junctions: molecular basis and pathological implications. Dev Cell 16, 209–221.

Dieckmann-Schuppert A, Schnittler H-J (1997). A simple assay for quantification of protein in tissue sections, cell cultures, and cell homogenates, and of protein immobilized on solid surfaces. Cell Tissue Res 288, 119–126.

Drees F, Pokutta S, Yamada S, Nelson WJ, Weis WI (2005). α-Catenin is a molecular switch that binds E-cadherin-β-catenin and regulates actin-filament assembly. Cell 123, 903–915.

Geyer H, Geyer R, Odenthal-Schnittler M, Schnittler HJ (1999). Characterization of human vascular endothelial cadherin glycans. Glycobiology 9, 915–925.

Halbleib JM, Nelson WJ (2006). Cadherins in development: cell adhesion, sorting, and tissue morphogenesis. Genes Dev 20, 3199–3214.

Helwani FM, Kovacs EM, Paterson AD, Verma S, Ali RG, Fanning AS, Weed SA, Yap AS (2004). Cortactin is necessary for E-cadherin-mediated contact formation and actin reorganization. J Cell Biol 164, 899–910.

Hetheridge C, Scott AN, Swain RK, Copeland JW, Higgs HN, Bicknell R, Mellor H (2012). The novel formin FMNL3 is a cytoskeletal regulator of angiogenesis. J Cell Sci 125, 1420–1428.

Hetrick B, Han MS, Helgeson LA, Nolen BJ (2013). Small molecules CK-666 and CK-869 inhibit actin-related protein 2/3 complex by blocking an activating conformational change. Chem Biol 20, 701–712.

Hoelzle MK, Svitkina T (2012). The cytoskeletal mechanisms of cell-cell junction formation in endothelial cells. Mol Biol Cell 23, 310–323.

Huveneers S, Oldenburg J, Spanjaard E, van der Krogt G, Grigoriev I, Akhmanova A, Rehmann H, de Rooij J (2012). Vinculin associates with endothelial VE-cadherin junctions to control force-dependent remodeling. J Cell Biol 196, 641–652.

Ichijima H, Petroll WM, Barry PA, Andrews PM, Dai M, Cavanagh HD, Jester JV (1993). Actin filament organization during endothelial wound healing in the rabbit cornea: comparison between transcorneal freeze and mechanical scrape injuries. Invest Ophthalmol Vis Sci 34, 2803–2812.

Iino R, Koyama I, Kusumi A (2001). Single molecule imaging of green fluorescent proteins in living cells: E-cadherin forms oligomers on the free cell surface. Biophys J 80, 2667–2677.

Kametani Y, Takeichi M (2007). Basal-to-apical cadherin flow at cell junctions. Nat Cell Biol 9, 92–98.

Kaverina I, Stradal TE, Gimona M (2003). Podosome formation in cultured A7r5 vascular smooth muscle cells requires Arp2/3-dependent de-novo actin polymerization at discrete microdomains. J Cell Sci 116, 4915–4924.

Kemper B, Bauwens A, Vollmer A, Ketelhut S, Langehanenberg P, Muthing J, Karch H, von Bally G (2010). Label-free quantitative cell division monitoring of endothelial cells by digital holographic microscopy. J Biomed Optics 15, 036009.

Kim SH, Li Z, Sacks DB (2000). E-cadherin-mediated cell-cell attachment activates Cdc42. J Biol Chem 275, 36999–37005.

Kitt KN, Nelson WJ (2011). Rapid suppression of activated Rac1 by cadherins and nectins during de novo cell-cell adhesion. PLoS One 6, e17841.

Kobielak A, Pasolli HA, Fuchs E (2004). Mammalian formin-1 participates in adherens junctions and polymerization of linear actin cables. Nat Cell Biol 6, 21–30.

Kovacs EM, Goodwin M, Ali RG, Paterson AD, Yap AS (2002). Cadherin-directed actin assembly: E-cadherin physically associates with the Arp2/3 complex to direct actin assembly in nascent adhesive contacts. Curr Biol 12, 379–382.

Kronstein R *et al.* (2012). Caveolin-1 opens endothelial cell junctions by targeting catenins. Cardiovasc Res 93, 130–140.

Lamalice L, Le Boeuf F, Huot J (2007). Endothelial cell migration during angiogenesis. Circ Res 100, 782–794.

Lampugnani MG, Corada M, Caveda L, Breviario F, Ayalon O, Geiger B, Dejana E (1995). The molecular organization of endothelial cell to cell junctions: differential association of plakoglobin, beta-catenin, and alpha-catenin with vascular endothelial cadherin (VE-cadherin). J Cell Biol 129, 203–217.

Lampugnani MG, Resnati M, Raiteri M, Pigott R, Pisacane A, Houen G, Ruco LP, Dejana E (1992). A novel endothelial-specific membrane protein is a marker of cell-cell contacts. J Cell Biol 118, 1511–1522.

Levesque MJ, Nerem RM (1985). The elongation and orientation of cultured endothelial cells in response to shear stress. J Biomech Eng 107, 341–347.

Li Y, Uruno T, Haudenschild C, Dudek SM, Garcia JG, Zhan X (2004). Interaction of cortactin and Arp2/3 complex is required for sphingosine-1-phosphate-induced endothelial cell remodeling. Exp Cell Res 298, 107–121.

Lie PPY, Chan AYN, Mruk DD, Lee WM, Cheng CY (2010). Restricted Arp3 expression in the testis prevents blood–testis barrier disruption during junction restructuring at spermatogenesis. Proc Natl Acad Sci USA 107, 11411–11416.

McKenzie JA, Ridley AJ (2007). Roles of Rho/ROCK and MLCK in TNF-alpha-induced changes in endothelial morphology and permeability. J Cell Physiol 213, 221–228.

Millan J, Cain RJ, Reglero-Real N, Bigarella C, Marcos-Ramiro B, Fernandez-Martin L, Correas I, Ridley AJ (2010). Adherens junctions connect stress fibres between adjacent endothelial cells. BMC Biol 8, 11.

Nelson WJ (2008). Regulation of cell-cell adhesion by the cadherin-catenin complex. Biochem Soc Trans 36, 149–155.

Noda K, Zhang J, Fukuhara S, Kunimoto S, Yoshimura M, Mochizuki N (2010). Vascular endothelial-cadherin stabilizes at cell-cell junctions by anchoring to circumferential actin bundles through α- and β-catenins in cyclic AMP-Epac-Rap1 signal-activated endothelial cells. Mol Biol Cell 21, 584–596.

Nolen BJ, Tomasevic N, Russell A, Pierce DW, Jia Z, McCormick CD, Hartman J, Sakowicz R, Pollard TD (2009). Characterization of two classes of small molecule inhibitors of Arp2/3 complex. Nature 460, 1031–1034.

Pober JS, Sessa WC (2007). Evolving functions of endothelial cells in inflammation. Nat Rev Immunol 7, 803–815.

Pollard TD (2007). Regulation of actin filament assembly by Arp2/3 complex and formins. Annu Rev Biophys Biomol Struct 36, 451–477.

Riedl J *et al.* (2008). Lifeact: a versatile marker to visualize F-actin. Nat Methods 5, 605–607.

Rorth P (2009). Collective cell migration. Annu Rev Cell Dev Biol 25, 407–429.

Rottner K, Hänisch J, Campellone KG (2010). WASH, WHAMM and JMY: regulation of Arp2/3 complex and beyond. Trends Cell Biol 20, 650–661.

Schneider CA, Rasband WS, Eliceiri KW (2012). NIH Image to ImageJ: 25 years of image analysis. Nat Methods 9, 671–675.

Schrot S, Weidenfeller C, Schaffer TE, Robenek H, Galla HJ (2005). Influence of hydrocortisone on the mechanical properties of the cerebral endothelium in vitro. Biophys J 89, 3904–3910.

Scott JA, Shewan AM, den Elzen NR, Loureiro JJ, Gertler FB, Yap AS (2006). Ena/VASP proteins can regulate distinct modes of actin organization at cadherin-adhesive contacts. Mol Biol Cell 17, 1085–1095.

Seebach J, Donnert G, Kronstein R, Werth S, Wojciak-Stothard B, Falzarano D, Mrowietz C, Hell SW, Schnittler HJ (2007). Regulation of endothelial barrier function during flow-induced conversion to an arterial phenotype. Cardiovasc Res 75, 596–607.

Seebach J, Madler HJ, Wojciak-Stothard B, Schnittler HJ (2005). Tyrosine phosphorylation and the small GTPase rac cross-talk in regulation of endothelial barrier function. Thromb Haemost 94, 620–629.

Shi SR, Shi Y, Taylor CR (2011). Antigen retrieval immunohistochemistry: review and future prospects in research and diagnosis over two decades. J Histochem Cytochem 59, 13–32.

Simionescu M, Simionescu N, Palade GE (1975). Segmental differentiations of cell junctions in the vascular endothelium. The microvasculature. J Cell Biol 67, 863–885.

Simionescu M, Simionescu N, Palade GE (1976). Segmental differentiations of cell junctions in the vascular endothelium. Arteries and veins. J Cell Biol 68, 705–723.

Suzuki S, Sano K, Tanihara H (1991). Diversity of the cadherin family: evidence for eight new cadherins in nervous tissue. Cell Regul 2, 261–270.
Vasioukhin V, Bauer C, Yin M, Fuchs E (2000). Directed actin polymerization is the driving force for epithelial cell-cell adhesion. Cell 100, 209–219.
Vestweber D, Winderlich M, Cagna G, Nottebaum AF (2009). Cell adhesion dynamics at endothelial junctions: VE-cadherin as a major player. Trends Cell Biol 19, 8–15.
Wahl-Jensen VM, Afanasieva TA, Seebach J, Stroher U, Feldmann H, Schnittler HJ (2005). Effects of Ebola virus glycoproteins on endothelial cell activation and barrier function. J Virol 79, 10442–10450.
Weis WI, Nelson WJ (2006). Re-solving the Cadherin-catenin-actin conundrum. J Biol Chem 281, 35593–35597.
Welch MD, Mullins RD (2002). Cellular control of actin nucleation. Annu Rev Cell Dev Biol 18, 247–288.
Wu C, Horowitz A (2011). Membrane traffic as a coordinator of cell migration and junction remodeling. Commun Integr Biol 4, 703–705.
Yamada S, Pokutta S, Drees F, Weis WI, Nelson WJ (2005). Deconstructing the cadherin-catenin-actin complex. Cell 123, 889–901.
Yonemura S (2011). Cadherin-actin interactions at adherens junctions. Curr Opin Cell Biol 23, 515–522.
Yuan D, He P (2012). Vascular remodeling alters adhesion protein and cytoskeleton reactions to inflammatory stimuli resulting in enhanced permeability increases in rat venules. J Appl Physiol 113, 1110–1120.